Static and dynamic properties of a viscous silica melt

Jürgen Horbach and Walter Kob
Institut für Physik, Johannes Gutenberg-Universität, Staudinger Weg 7, D-55099 Mainz, Germany
(Received 20 January 1999)

We present the results of a large scale molecular dynamics computer simulation in which we investigated the static and dynamic properties of a silica melt in the temperature range in which the viscosity of the system changes from $O(10^{-2})$ P to $O(10^{2})$ P. We show that even at temperatures as high as 4000 K the structure of this system is very similar to the random tetrahedral network found in silica at lower temperatures. The temperature dependence of the concentration of the defects in this network shows an Arrhenius law. From the partial structure factors we calculate the neutron scattering function and find that it agrees very well with experimental neutron scattering data. At low temperatures the temperature dependence of the diffusion constants D shows an Arrhenius law with activation energies which are in very good agreement with the experimental values. With increasing temperature we find that this dependence shows a crossover to one which can be described well by a power law, $D \propto (T-T_c)^{\gamma}$. The critical temperature T_c is 3330 K and the exponent γ is close to 2.1. Since we find a similar crossover in the viscosity, we have evidence that the relaxation dynamics of the system changes from a flowlike motion of the particles, as described by the ideal version of mode-coupling theory, to a hoppinglike motion. We show that such a change of the transport mechanism is also observed in the product of the diffusion constant and the lifetime of a Si-O bond or the space and time dependence of the van Hove correlation functions. [S0163-1829(99)01329-6]

I. INTRODUCTION

In recent years the dynamics of supercooled liquids has been the focus of many investigations and due to these efforts our understanding of this dynamics has increased significantly. Although very recently new interesting phenomena in this dynamics have been found, such as dynamical heterogeneities[1] or the aging dynamics of the system at very low temperatures,[2] which so far are not understood, we have by now at least a fair understanding of the relaxation dynamics at temperatures a bit above the experimental glass transition temperature T_g. In particular it has been demonstrated that the so-called mode-coupling theory (MCT),[3] a theory which relates the slowing down of the dynamics upon cooling to nonlinear feedback effects, is able to give a qualitative and quantitative correct description of glass formers in which the interaction between particles is not too different from the one of a hard-sphere system, such as colloidal systems,[4] the molecular glass-former orthoterphenyl,[5] and even systems in which some hydrogen bonding is present, such as glycerol.[6] The main prediction of the theory is that there exists a critical temperature T_c at which the relaxation dynamics of the system changes qualitatively in that an unexpectedly fast increase of the local activation energy of the transport coefficients, such as the viscosity or the inverse of the diffusion constant, is observed. Qualitatively such a temperature dependence can readily be seen in the so-called Angell plot,[7] where the logarithm of the viscosity is plotted versus T_g/T, in that the so-called fragile glass formers show, at around $(1.1–1.3)T_g$, a sharp upward bend. Because of the similarity between this bend and the prediction of MCT, many investigations on the dynamics of glass formers have been done for these types of systems, so that the validity of the theory could be checked. Apart from this, most fragile systems have glass transition temperatures which are readily accessible in an experiment, thus making it relatively simple to investigate the dynamics at and above T_g. This is not the case for most *strong* glass formers, since their T_g is often above 500 K, such as SiO_2, B_2O_3, or GeO_2, to name a few. Because of their high value of T_g the *microscopic* dynamics of these systems is understood in much less detail than the one of fragile glass formers. Sidebottom *et al.*[8] have investigated the dynamics of B_2O_3 by means of photon correlation spectroscopy, and very recently Wischnewski *et al.*[9] have used neutron scattering experiments to study the dynamics of SiO_2 also at high temperatures. Despite these investigations our knowledge of the dynamics of strong glass formers is significantly less than that of fragile ones.

Valuable insight into the dynamics of supercooled liquids has also been obtained through computer simulations. Whereas many of the earlier studies[10] have investigated the dynamics of strong glass formers, most of the more recent studies focused on simple liquidlike systems, such as soft spheres or Lennard-Jones systems, since in the latter type of models the interaction between the particles is much simpler than in that of strong glass formers and hence the system can be probed in larger time windows. Very recently, however, the investigation of strong glass formers, mainly silica, by means of computer simulations has become more popular again. From such simulations it is hoped that insight is gained into, e.g., the nature of the so-called boson peak,[11–13] a dynamical feature at around 1 THz whose origin is still a matter of debate,[9,14] or to investigate the structure and dynamics at different pressures and temperatures on a microscopic level.[15]

Despite the mentioned investigations we are, however, still lacking a comparable detailed characterization of the relaxation dynamics of strong glass formers as has been obtained for simple liquids[16–19] and water.[20] In the present work we therefore present the results of a molecular dynam-

ics computer simulation of silica, the prototype of a strong glass former, in which such an analysis has been done. These results will allow us to gain more insight into the dynamics of this system, to relate it to its structural properties, and to compare these results with the ones obtained for fragile systems. The rest of the paper is organized as follows: In Sec. II we give the details of the model and the simulation, in Sec. III we present the results, and in Sec. IV we summarize and discuss them.

II. MODEL AND DETAILS OF THE SIMULATIONS

As already mentioned in the Introduction, various aspects of the dynamics of amorphous silica have already been investigated. In these simulations potentials with different levels of accuracy have been used, most of which give a satisfactory description of the *structural* (i.e., static) properties of amorphous silica. Very recently Hemmati and Angell have pointed out, however, that the predictions of these various potentials regarding *dynamical* properties, such as the diffusion constant at low temperatures, can differ by orders of magnitudes.[21] For the investigation of the dynamical behavior it is therefore important to choose the potential with particular care. One of the most reliable potentials seems to be the one proposed by van Beest, Kramer, and van Santen (BKS) which was developed by using a mixture of *ab initio* calculations and classical lattice dynamics simulations.[22] The BKS potential is given by

$$\phi(r)=\frac{q_\alpha q_\beta e^2}{r}+A_{\alpha\beta}\exp(-B_{\alpha\beta}r)-\frac{C_{\alpha\beta}}{r^6}. \qquad (1)$$

Here r is the distance between two ions of type α and β ($\alpha,\beta\in\{\mathrm{Si, O}\}$) and the values of the partial charges q_α and the constants $A_{\alpha\beta}$, $B_{\alpha\beta}$, and $C_{\alpha\beta}$ can be found in Refs. 22 and 23. As we have already done in previous investigations of this model,[13,23–27] we have truncated and shifted the non-Coulombic part of this potential at a cutoff radius of 5.5 Å. This modification of the potential has the positive effect that at normal pressure the density of the glass is around 2.3 g/cm^3, a value that is very close to the one of real silica glass, 2.2 g/cm^3.[28] In previous work we have found that the dynamics of strong glass formers shows quite significant finite size effects.[25] In order to avoid them we used a system which is relatively large for simulation of supercooled liquids, i.e., 8016 ions. During the runs the size of the cubic simulation box was fixed to $L=48.37$ Å. Thus the density of the system was kept constant at 2.37 g/cm^3, which leads to a pressure which is a bit above normal pressure (discussed in more detail below).

The Coulombic part of the potential was evaluated by means of Ewald sums with a constant $\alpha L=12.82$ (Ref. 29) and by using for the Fourier part of the Ewald sum all k vectors of magnitude less than $k_c=2\pi\sqrt{51}/L$. A short calculation shows that, although such a small value of k_c is sufficient to calculate the interaction between two ions to a satisfactory accuracy, it would be insufficient to set the *absolute* error of the *total* Coulombic energy below an acceptable level. However, it can be shown,[30] that this small value of k_c leads just to a constant shift of the energy scale and hence does not affect the forces.

Using the potential given by Eq. (1) and the masses of 28.086 u and 15.9994 u for the silicon and oxygen atoms, respectively, we equilibrated the system by doing a *NVT* simulation (temperature was kept constant by means of a stochastic collision algorithm). At each temperature investigated, we made sure that the length of these equilibration runs exceeded the typical relaxation times of the system. The temperatures considered were 6100 K, 5200 K, 4700 K, 4300 K, 4000 K, 3760 K, 3580 K, 3400 K, 3250 K, 3100 K, 3000 K, 2900 K, and 2750 K. In order to improve the statistics of the results we averaged at each temperature over two independent runs. After the equilibration we started microcanonical runs by integrating the equations of motion with the velocity form of the Verlet algorithm. The time step used was 1.6 fs, which is sufficiently small to guarantee a negligible drift of the total energy of the system at high and intermediate temperatures (6100 K$\geqslant T\geqslant$3100 K) over the whole run. For the lowest temperatures ($T\leqslant$3000 K) the runs were so long that the drift in the energy could no longer be neglected.[31] Therefore we rescaled every 1×10^6 time steps the velocity of the particles to bring the system back to the energy at which it was started. This frequency should be small enough to avoid any effect on the relaxation dynamics. At the lowest temperature the length of the runs were 12×10^6 time steps (and 13×10^6 for the equilibration), giving a total simulation time of about 20 ns. The overall computational effort (equilibration plus production) for this temperature was about 13 years of single processor time on a CRAY-T3E (or 2.5 months on 64 processors).

III. RESULTS

In order to understand the dynamical behavior of the system it is useful to know something about its static properties since we will show that the transport mechanism of the atoms is intimately related to the network structure of the system. Therefore we present in the following subsection some of the static properties before we discuss in the subsequent subsection the dynamics of the system.

A. Static properties

One of the most remarkable properties of amorphous silica is that it shows a density anomaly at around 1820 K.[28] Although in a constant volume simulation such an anomaly can of course not be observed in the density, it can easily be seen in the temperature dependence of the pressure p, which is shown in Fig. 1. We see that after a fast decrease of p between 6100 K and 5200 K, the pressure reaches a minimum at around 4900 K, thus showing that the density at constant pressure has a maximum, and then increases again with decreasing temperature. Since the experimental value at which this density anomaly occurs is 1820 K,[28] we confirm the result of the constant pressure simulation,[23] that the BKS potential overestimates the temperature at which the density anomaly is observed.

That this extremum in pressure is not accompanied by a significant change in the structural quantity $g_{\alpha\beta}$, the partial radial distribution functions between particles of type α and β,[32] is demonstrated in Fig. 2, where we show the three $g_{\alpha\beta}$ for three different temperatures. What can also be recognized from these figures is that the BKS model predicts that even at

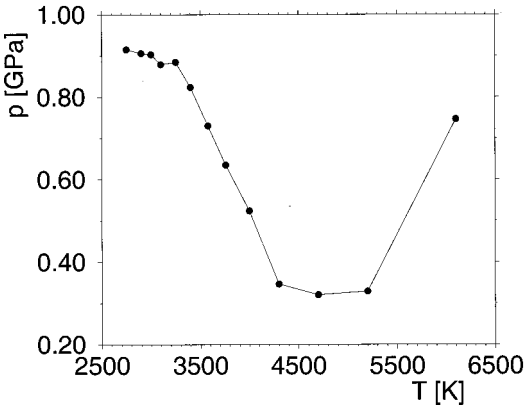

FIG. 1. Temperature dependence of the pressure.

a temperature of 6100 K the arrangement of the particles shows a structure which is much more similar to the one of a liquid at its triple point than to the one of a gas. It should be realized that this result is not in contradiction with the experimental result that a silica melt at several thousand kelvin does evaporate, *if a free surface is present*. We have found that if the geometry of the simulation does contain such a free surface, the BKS model also predicts that the atoms will evaporate from the system.[33] However, due to the presence of the periodic boundary, no free surface is present in the simulation discussed in this work and thus no evaporation takes place.

We also remark that in the temperature range considered, the time scale of the relaxation dynamics of the system changes by about four decades (this will be discussed in the next subsection). Thus we find that a *relatively* small change in the structure of the melt is accompanied by a dramatic change in the dynamics, an observation which is qualitatively similar to the one found for simple liquids.[16–19] This fact thus gives support to the point of view put forward by the mode-coupling theory,[3] which predicts that although the temperature dependence of all structural quantities of a supercooled melt is very weak, most dynamical quantities connected to the density fluctuations of the system will show a very strong temperature dependence. Below we will discuss these aspects in more detail.

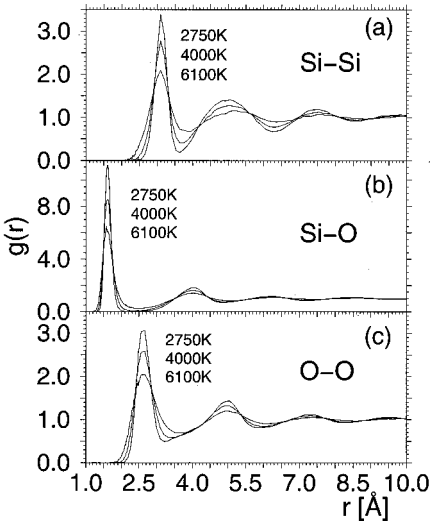

FIG. 2. Radial distribution functions for different temperatures. (a) Si-Si, (b) Si-O, and (c) O-O.

From the figure we also recognize that for all temperatures there is a well-defined minimum between the first and second peaks. Therefore it is possible to identify for each ion its nearest neighbors by requiring that they be within the first nearest neighbor shell, defined by the location of the mentioned minimum. For the following analysis we used the values 3.64 Å, 2.35 Å, and 3.21 Å for the location of this minimum in the Si-Si, Si-O, and O-O correlations. In Fig. 3 we show the probability $P_{\alpha\beta}$ that a ion of type α has exactly z nearest neighbors of type β, for all relevant values of z. From Figs. 3(a) and 3(b) we recognize that even at high temperatures more than 85% of the silicon and oxygen atoms are fourfold and twofold coordinated, respectively, i.e., that they are in the local environment expected from an ideal (corner-shared) tetrahedral network. At the lowest temperature investigated this fraction is higher than 99%. The remaining defects are silicon atoms that are threefold and fivefold coordinated and oxygen atoms that are threefold and onefold coordinated, the latter thus forming dangling bonds. We have found that for temperatures below 3700 K the probability for the occurrence of such defects is described very well by an Arrhenius law $P_{\alpha\beta}=\pi_{\alpha\beta}\exp(-e_{\alpha\beta}/T)$ (dashed curves). As prefactors $\pi_{\alpha\beta}$ and activation energies $e_{\alpha\beta}$ we found $\pi_{\mathrm{SiO}}=4.4$, $e_{\mathrm{SiO}}=17130$ K for $z=5$, $\pi_{\mathrm{SiO}}=58.6$, $e_{\mathrm{SiO}}=31100$ K for $z=3$, $\pi_{\mathrm{OSi}}=3.2$, $e_{\mathrm{OSi}}=17730$ K for $z=3$, and $\pi_{\mathrm{OSi}}=8.9$, $e_{\mathrm{OSi}}=24760$ K for $z=1$. From these activation energies we recognize that at low temperatures defects in which a silicon atom is coordinated by $z=5$ oxygen atoms or one in which an oxygen atom is bound to $z=3$ silicon atoms are by far the most frequent ones. In Refs. 23 and 34 it was shown that once the system has reached the glass transition temperature, the distributions P_{SiO} and P_{OSi} do not change anymore, i.e., that at low temperatures these distributions are given by the ones at the glass transition temperature. By using the above given activation energies we can therefore extrapolate the curves to the experimental value of T_g and thus estimate the density of the defects of real silica below T_g. Using the value $T_g=1450$ K,[28] we predict that fivefold-coordinated silicon atoms occur with probability 3.2×10^{-5} and threefold-coordinated oxygen atoms with probability 1.5×10^{-5}.

Whereas the temperature dependence of the Si-O and O-Si defects is quite simple, we see from Figs. 3(c) and 3(d) that this is not the case for the defects involving the structure on somewhat larger length scales, since the functional form of the various curves is not easy to identify. Thus the main information that can be obtained from these figures is that locally the system seems to approach the geometry of a random tetrahedral network. In this structure the most probable configuration is that an oxygen atom has six other oxygen atoms as its second nearest neighbors and a silicon atom has four other silicon atoms as its second nearest neighbors.

The structure at larger length scales can best be studied by means of the partial structure factors $S_{\alpha\beta}(q)$,[32], since any large scale feature will show up at wave vectors q which are smaller than the location of the peak between neighboring particles, i.e., in our case the Si-O correlation. In Fig. 4 we show the three $S_{\alpha\beta}(q)$ for the same temperatures already

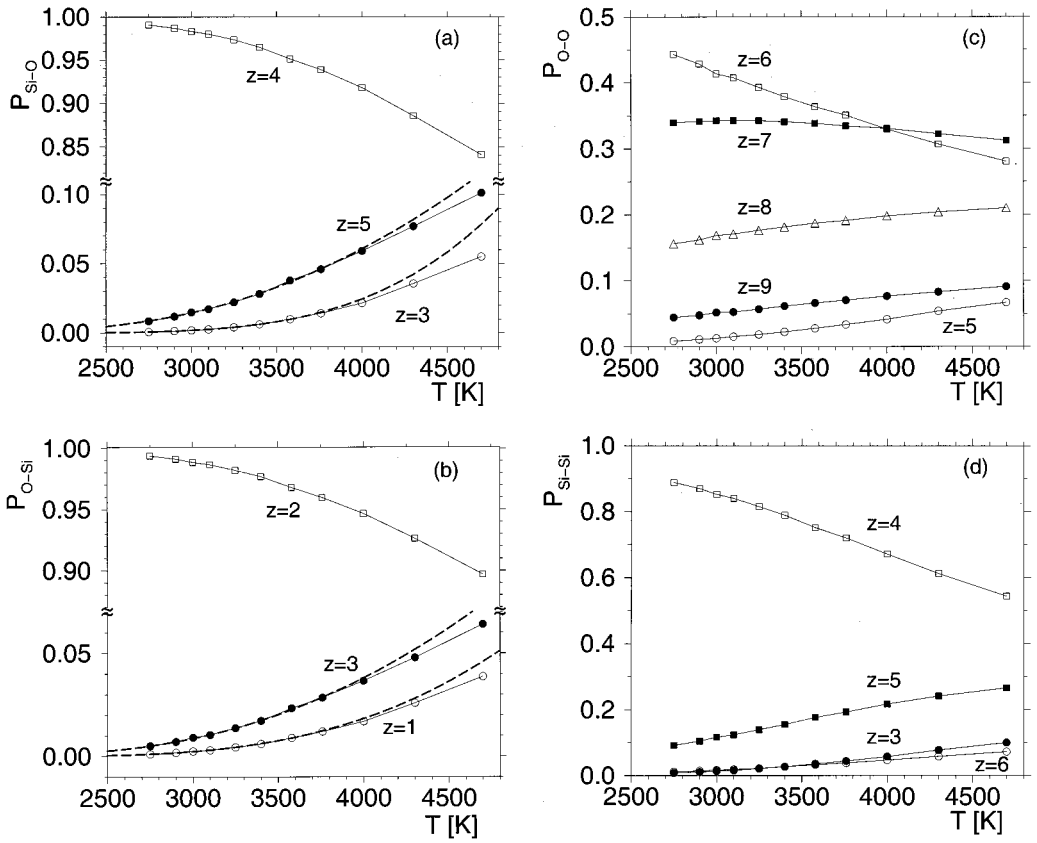

FIG. 3. Temperature dependence of the partial coordination numbers z. The dashed lines in (a) and (b) are fits with an Arrhenius law. (a) $P_{\text{Si-O}}$, (b) $P_{\text{O-Si}}$, (c) $P_{\text{O-O}}$, and (d) $P_{\text{Si-Si}}$.

discussed in Fig. 2. The peak corresponding to the nearest neighbor Si-O distance is around 2.8 Å^{-1}. At smaller wave vectors an additional peak can be seen, the so-called first sharp diffraction peak (FSDP). The microscopic reason for this peak is the local chemical ordering of the ions in tetrahedra-like structures and the location of the peak is related to the distance between neighboring tetrahedra. The interesting information that can be obtained from Fig. 4 is that the FSDP is observed already at temperatures as high as 4000 K. At first glance it might seem a somewhat unrealistic prediction of the BKS model that the open structure of the network should be present even at such high temperatures. However, if one recalls that even at temperatures as high as 2750 K silica is a quite viscous liquid ($\eta \approx 2000$ P),[35] this result is no longer that surprising, since such a high value of the viscosity shows that even at these high temperatures the particles move quite slowly and that therefore their motion is strongly hindered by their neighbors. Therefore it is not surprising that the different $S_{\alpha\beta}(q)$ show that there is indeed a lot of structure in the system even at high temperatures.

Also included in Fig. 4 are curves for $T=300$ K. These were obtained by using the equilibrated configurations at $T=2900$ K as starting configurations of a cooling run in which the temperature was decreased linearly within 1×10^6 time steps to 0 K. This corresponds to a cooling rate of about 1.8×10^{12} K/s. With this cooling rate the system falls out of equilibrium at around 2850 K and thus this temperature corresponds to about the value of the fictive temperature of the glass. The configurations that we obtained at $T=300$ K were annealed for another 500 000 time steps before we started to calculate the structure factors. From the figure we recognize that the partial structure factors for this temperature seem to evolve very smoothly from the (equilibrium) ones at higher temperature, which however, is not quite correct, as we will demonstrate below.

In order to compare our results for the structure factors with the one of real silica we have also calculated the neutron scattering function $S_n(q)$ from

$$S_n(q)=\frac{1}{N_{\text{Si}}b_{\text{Si}}^2+N_{\text{O}}b_{\text{O}}^2}\sum_{k,l}^{N} b_k b_l \langle \exp[i\mathbf{q}\cdot(\mathbf{r}_k-\mathbf{r}_l)]\rangle, \quad (2)$$

where $b_k, k\in\{\text{Si,O}\}$, are the neutron scattering cross sections, and $\langle\cdot\rangle$ is the thermal average. Susman *et al.*[36] report for b_{Si} and b_{O} the values 0.4149×10^{-12} cm and 0.5803×10^{-12} cm, respectively. Using these values and Eq. (2) we obtain for $T=300$ K the $S_n(q)$ shown in Fig. 5. Also included in the figure is the neutron scattering result of Price and Carpenter at the same temperature.[37] We recognize that qualitatively, as well as quantitatively, the two curves agree very well, in that not only the location, but also the height of the various peaks is reproduced well. This shows that the BKS potential is indeed able to reproduce this structural quantity. A similar good agreement was obtained by Taraskin and Elliott who calculated $S_n(q)$ for SiO_2 within the harmonic approximation.[12] One significant difference between the theoretical and experimental curves can, however, be noticed, and this is their behavior at small wave vectors. Whereas an extrapolation of the theoretical curve to $q=0$ seems to give a value around 0.16, the experimental curve

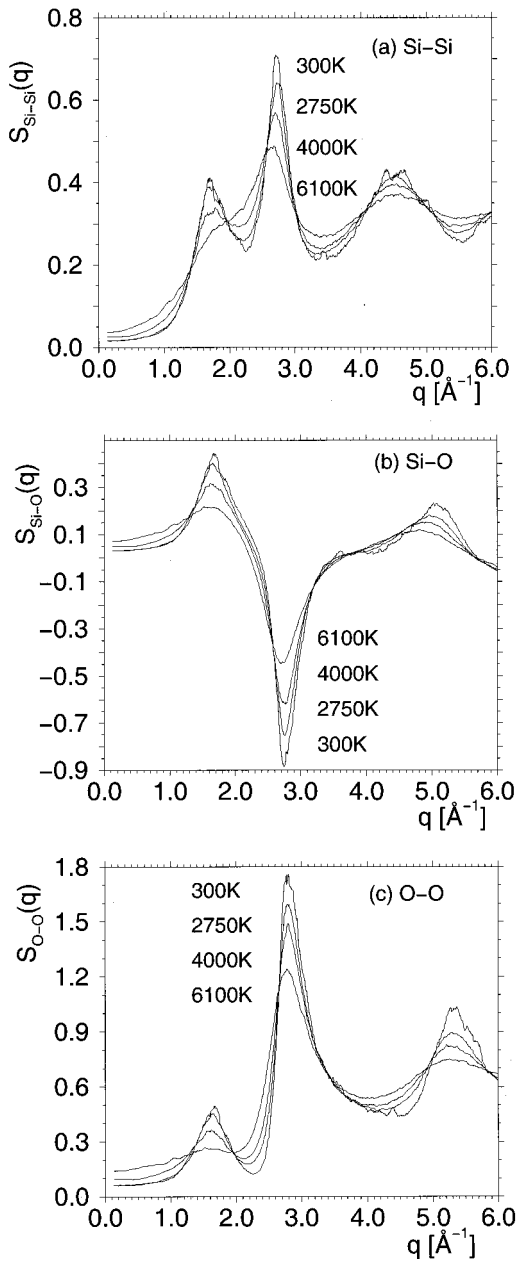

FIG. 4. Partial structure factors $S_{\alpha\beta}(q)$ for different temperatures. The curves for 300 K were obtained by quenching the system from a high-temperature state and are therefore not equilibrium curves. (a) Si-Si, (b) Si-O, and (c) O-O.

seems to extrapolate to a significantly smaller value. It is well known that this value of the *total* structure factor,

$$S(q)=N^{-1}\sum_{k,l=1}^{N}\langle\exp[i\mathbf{q}\cdot(\mathbf{r}_k-\mathbf{r}_l)]\rangle, \tag{3}$$

is related to the isothermal compressibility κ_T of the system via

$$\lim_{q\to 0}S(q)=\rho k_B T\kappa_T, \tag{4}$$

where $\rho=N/V$ is the particle density. We therefore extrapolated our partial structure factors to $q=0$ and thus obtained $S(q)$ for $q\to 0$. This quantity is shown in Fig. 6 as a function of temperature. We see that as long as we are in equilibrium, $T\geqslant 2750$ K, $S(q=0)$ decreases continuously with decreasing temperature. At our (computer) glass transition $T\approx 2850$ K, however, the structure freezes in and thus, at $T=300$ K, $S(q=0)$ is essentially given by its value at this glass transition temperature.[38] Thus we see that it is not surprising that in Fig. 5 the theoretical curve at small wave vectors is above the experimental one.

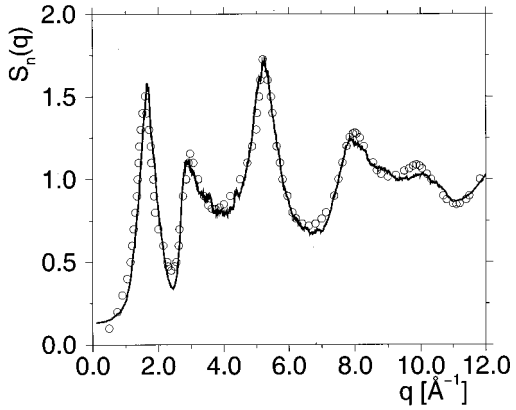

FIG. 5. Comparison of the neutron scattering function from our simulation (solid line) with the experimental data of Price and Carpenter (Ref. 37) (circles).

In the inset of Fig. 6 we show the compressibility of our system as calculated from Eq. (4). We see that also this quantity has a maximum at a temperature which corresponds to the location of the density anomaly of the system, i.e., for this model at around 4700 K. No experimental data for κ_T in this temperature range are known to us. However, Fraser[39] reports for $T=1673$ K a compressibility around 2.7×10^{-5} GPa^{-1}. If we extrapolate the (equilibrium) compressibility data in Fig. 6 to $T=1673$ K, we obtain a κ_T at around 1.35×10^{-5} GPa^{-1} which is a factor of 2 smaller than the one given by Fraser. Thus we have evidence that the BKS model is a bit too stiff. The possibility that this discrepancy is due to the slightly enhanced pressure of our system should, however, not be disregarded.

B. Dynamic properties

Having studied the static properties of the silica melt we will discuss in this subsection the dynamic ones.

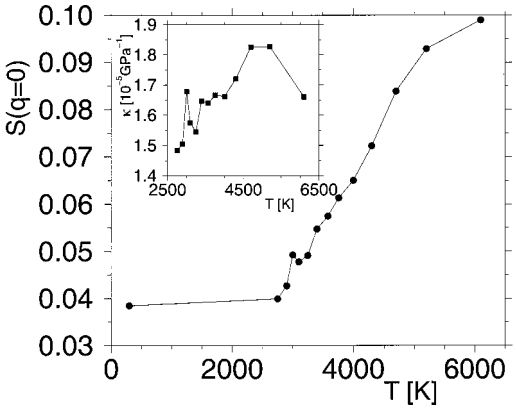

FIG. 6. Main figure: value of the total structure factor at $q=0$ as a function of temperature. Inset: temperature dependence of the compressibility.

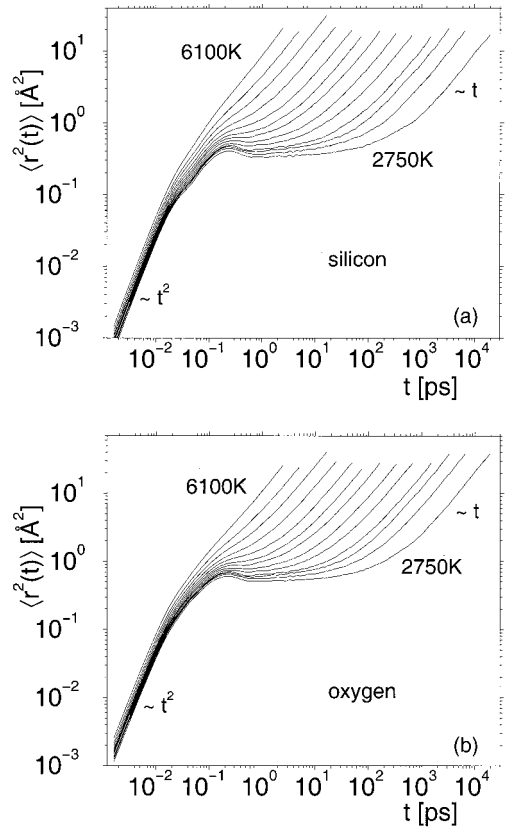

FIG. 7. Time dependence of the mean squared displacement for different temperatures, (a) silicon and (b) oxygen.

One of the simplest quantities to study the dynamics of a fluid system on a microscopic level is the mean-squared displacement (MSD) $\langle r^2(t)\rangle$ of a tagged particle (of type α), which is given by

$$\langle r^2(t)\rangle = \frac{1}{N_\alpha}\sum_{l=1}^{N_\alpha}\langle|\mathbf{r}_l(t)-\mathbf{r}_l(0)|^2\rangle. \tag{5}$$

The time dependence for this quantity is shown in Fig. 7 for all temperatures investigated. For high temperatures, curves to the left, two time regimes can be distinguished. At short times the motion of the particles is ballistic, i.e., $\mathbf{r}_l(t) \approx \mathbf{r}_l(0)+\dot{\mathbf{r}}_l t$, and the MSD is proportional to t^2. For long times the motion is diffusive and hence we have $\langle r^2(t)\rangle \propto t$. These two regimes are also seen at low temperatures, curves to the right. However, at these temperatures these two regimes are separated by a third one, in which the MSD does not change significantly over a time span which extends over several decades in time. The microscopic reason for this behavior is the so-called cage effect, i.e., the fact that in this time regime the tagged particle is temporarily trapped by the particles surrounding it and hence make an escape from its cage very unlikely. Only for a sufficiently large time does the particle succeed in escaping this (dynamic) cage and the MSD starts again to increase significantly. The dynamics of the particles related to this cage is usually called the β relaxation and the mentioned mode-coupling theory makes detailed predictions about this dynamics, as will be discussed in more detail below.

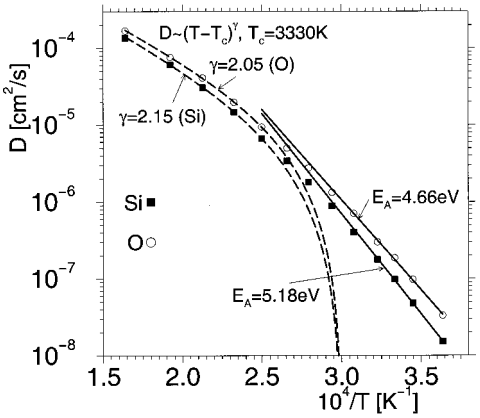

FIG. 8. Arrhenius plot of the diffusion constants. Bold solid lines: Arrhenius fits to the data at low temperatures with the stated activation energies. Dashed lines: results of a fit to the high-temperature data with the power law predicted by MCT with a critical temperature of 3330 K.

What is also noticeable in the curves at low temperatures is that the transition from the ballistic to the cage regime is quite different from the one found in a simple liquid (see, e.g., Ref. 19), in that (i) immediately after the ballistic regime the curves show a small shoulder at around 0.03 ps and (ii) a peak is observed at around 0.2 ps. The first of these features, which is more pronounced in the curves for the silicon atoms, is most likely the result of the complex *local* motion of the atoms in the open tetrahedral network, such as the bending and stretching of the tetrahedra. The second one is, as already pointed out by Angell *et al.*[40], related to the so-called boson peak, a vibrational feature at low frequencies whose precise origin is currently still a matter of debate.[12–14]

We also point out that the above-mentioned cage effect becomes observable already at temperatures as high as 3580 K. Usually this effect is associated with the glass former being in a *supercooled* state. However, since the melting temperature T_m of silica is around 2000 K, all our simulations are above T_m and hence we do not investigate the system in its supercooled regime at all. This shows that the melting temperature is, from the point of view of the cage effect, an irrelevant temperature. That this somewhat surprising result is not a particularity of the silica model studied here can be inferred from the fact that experimental studies of glycerol and B_2O_3 also show a strong non-Debye relaxation at temperatures well above their melting temperature.[6,41] All these results give support to the point of view of the earlier mentioned MCT, that the whole slowing down of the system is a purely kinetic phenomenon and thus not related to any thermodynamic singularity of any kind.

Using the Einstein relation $\lim_{t\to\infty}\langle r^2(t)/6t\rangle = D$, it is easy to calculate the diffusion constants D from the MSD. These are plotted in Fig. 8 as a function of the inverse temperature. As expected for a strong glass former, we find that at low temperatures the diffusion constants show an Arrhenius dependence. The activation energies are 4.66 eV and 5.18 eV for oxygen and silicon, respectively (bold solid lines). These numbers compare very well with the ones determined in experiments at significantly lower temperatures, namely, 4.7 eV for oxygen[42] and 6 eV for silicon.[43] That such an excellent agreement between the theoretical and experimen-

tal activation energies is not trivial has recently been demonstrated by Hemmati and Angell,[21] who showed that various models for silica can give rise to quite different activation energies. These authors also showed that the different models predict diffusion constants which differ by up to two decades at temperatures as high as 3000 K, which shows that dynamical quantities like D depend much more sensitively on the potential than structural quantities.

For higher temperatures we see from the figure that significant deviations from the Arrhenius behavior are observed in that the diffusion constants increase slower with increasing temperature than expected from an activated process. A similar change in the temperature dependence of D has also been found in many other models for silica.[21] Recently Hess *et al.* have reported the analysis of experimental viscosity data of SiO_2 at high temperatures and find that deviations from a pure Arrhenius law are present.[44]

One explanation to rationalize the observed deviations from the Arrhenius behavior is offered by MCT,[3] since the so-called ideal version of this theory predicts that the temperature dependence of the diffusion constant, as well as the inverse of the α-relaxation time $\tau(T)$, is given by a power law, i.e.,

$$D \propto \tau^{-1} \propto (T - T_c)^{\gamma}, \tag{6}$$

where the critical temperature T_c and the critical exponent γ can, in principle, be calculated from the temperature dependence of the partial structure factors. In practice, however, the two quantities are usually taken as fit parameters[3] (for exceptions see Ref. 45 and references therein). Instead of using the diffusion data alone to determine γ and T_c, it has been found in similar types of analysis (e.g., Refs. 18–20 and 46) that more reliable results are obtained if one determines these quantities from simultaneous fits to the diffusion constants as well as to the α-relaxation times for different wave vectors, and therefore we proceeded in this way too.[47] The result of these fits is that the critical temperature is 3330 K. This value of T_c is in excellent agreement with the one determined by Hess *et al.* in their analysis of viscosity data of real silica, which is 3221 K.[44] (We note that we have learned about the results of Hess *et al.* only after having determined our value of T_c.) Using our value of T_c, we obtain for the critical exponent γ the values 2.15 and 2.05 for the silicon and oxygen diffusion constants, respectively. Note that the theory predicts that the value of γ should be independent of the species and the fact that the two values we find are so close together supports this prediction. The so-obtained power-law fits are included in Fig. 8 as well and we see that they give a good description of the diffusion constants over about 1.5 decades in D. This range is significantly smaller than the one found in the case of simple liquids for which the power law can be observed over about three decades.[17,18] As substantiated below, the reason for this relatively small range is very likely the fact that in SiO_2 the relaxation dynamics at low temperatures is dominated by strong hopping processes, i.e., jump like motions of the ions. Since the *ideal* version of MCT, i.e., the version that predicts the power law given by Eq. (6), does not take into account these types of processes, it is thus not surprising that this version of the theory is applicable only in a quite limited temperature range. The solution to this problem might be the so-called extended MCT, i.e., that version of the theory in which such hopping processes are taken into account.[3,48] Since, however, so far the details of this theory for the α relaxation have not been worked out, no test can presently be made. This situation is different in the β-relaxation regime, where some of the predictions of the extended MCT have been worked out and, as we will demonstrate in a different place,[47] that these predictions hold very well for the present system.

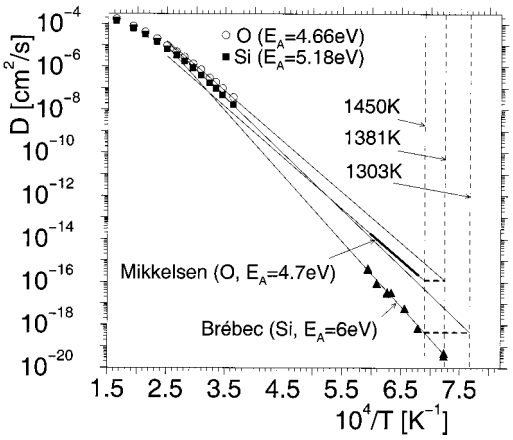

FIG. 9. Arrhenius plot of the diffusion constants as determined from our simulation (open circles, oxygen; solid squares, silicon) and the experimental values for oxygen (bold line) (Ref. 42) and silicon (Ref. 43). Thin solid lines: extrapolation of our data to low temperatures and extrapolation of the experimental data to high temperatures. See text for the discussion of the other lines.

Although Fig. 7 suggests that MCT might be useful to describe the dynamics of the present system, the power-law fits in Fig. 8 are of course not a proof that the extracted parameters T_c and γ have a deep physical meaning. The significance of the theory for SiO_2 becomes only obvious if also the α- and β-relaxation dynamics of the time correlation functions are analyzed carefully, which is done in Refs. 30 and 47. We mention already at this place, however, that the value for the critical exponent found for the diffusion constant, $\gamma \approx 2.1$, is slightly smaller than the one found for the α-relaxation time τ for larger wave vectors, which is around 2.35.[47] The value of this latter exponent is compatible with the relation proposed by MCT between these critical exponents and the value of the so-called von Schweidler exponent of the β-relaxation regime. Hence we conclude that the critical exponent of the diffusion constant is smaller than expected from MCT, an observation which is in agreement with the one made for simple liquids.[18,49]

Having now presented the temperature dependence of the diffusion constants in the temperature range of our simulation, it is instructive to compare these results with the ones of real experiments. For this we show in Fig. 9 the diffusion constants as measured by us and the ones determined in experiments by Mikkelsen[42] and by Bréebec *et al.*[43]. Also included are the Arrhenius fits to our data. We see that the extrapolation of these fits to the temperature range which is accessible to the experiments overestimates the diffusion constant by about one decade in the case of oxygen and by about two decades in the case of silicon. From such a plot we can also estimate the temperature at which the BKS model

would show the *experimental* glass transition temperature T_g, if we would have access to computers which are by about a factor of 10^{10} faster. For this we read off the experimental values of the diffusion constants at the experimental $T_g = 1450$ K (horizontal dashed lines) and determine the temperatures at which the Arrhenius extrapolation of our data crosses these values. From this construction we obtain a $T_{g,sim}$ of 1380 K and 1303 K for oxygen and silicon, respectively (vertical dashed lines). Thus we come to the remarkable conclusion that using the BKS potential it is possible to estimate the experimental glass transition temperature to within 10%.

Another important transport quantity is the shear viscosity η. Since η is a collective quantity, it is quite demanding to measure it in a simulation with high accuracy. For the case of silica the only simulation we know in which η has been determined is the one by Barrat *et al.* in which the pressure and temperature dependence of the viscosity was determined at relatively high temperatures.[50]

As in the case of the diffusion constant there are two possibilities to calculate η: from a Green-Kubo relation and a generalized Einstein relation.[51] The Green-Kubo relation is

$$\eta = \frac{1}{k_B T V} \int_0^\infty dt \langle \dot{A}_{\alpha\beta}(t) \dot{A}_{\alpha\beta}(0) \rangle, \tag{7}$$

where the off-diagonal elements of the pressure tensor are given by

$$\dot{A}_{\alpha\beta} = \sum_{i=1}^{N} m_i v_i^\alpha v_i^\beta + \sum_{i=1}^{N} \sum_{j>i}^{N} F_{ij}^\alpha r_{ij}^\beta, \quad \alpha \neq \beta. \tag{8}$$

Here F_{ij}^α is the α component of the force between ions i and j.

The Einstein formula reads

$$\eta = \frac{1}{k_B T V} \lim_{t\to\infty} \langle [A_{\alpha\beta}(t) - A_{\alpha\beta}(0)]^2 \rangle, \tag{9}$$

with

$$A_{\alpha\beta}(t) = \sum_{i=1}^{N} m_i v_i^\alpha(t) r_i^\beta(t). \tag{10}$$

Allen *et al.* have pointed out that in order to obtain correct results it is important to represent the term $A_{\alpha\beta}(t) - A_{\alpha\beta}(0)$ in Eq. (9) in a way which is independent of the coordinate system.[52] One possible choice is

$$A_{\alpha\beta}(t) - A_{\alpha\beta}(0) = \int_0^t dt' \dot{A}_{\alpha\beta}(t'). \tag{11}$$

We also mention that care has also been taken in the evaluation of the forces F_{ij}^α occurring in Eq. (8), since it is not possible to use just the ones obtained from the Ewald sums. More details on this problem can be found in Ref. 53. In the course of our calculation we found that the two methods discussed to calculate η give results with similar accuracy, and thus can be considered to be equivalent from a numerical point of view.

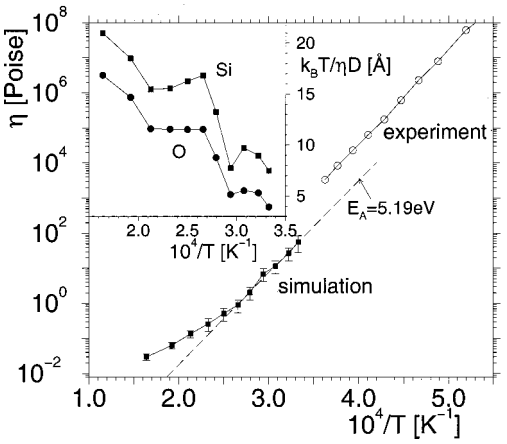

FIG. 10. Main figure: Arrhenius plot of the shear viscosity from the simulation (solid squares). The dashed line is a fit with an Arrhenius law to our low-temperature data. The open circles are experimental data from Urbain *et al.* (Ref. 35). Inset: temperature dependence of the left hand side of Eq. (12) to check the validity of the Stokes-Einstein relation.

Because of the mentioned collective nature of η, the usual two runs we did at every temperature were not sufficient to allow to determine η with a satisfactory statistical accuracy. Therefore we performed, for all temperatures above 2900 K, 18 extra runs in order to calculate η. Because of the long relaxation times at $T = 2900$ K and $T = 2750$ K, it was not possible to do that many runs at these temperatures and thus no results for η have been obtained.

In Fig. 10 we show the temperature dependence of the viscosity in an Arrhenius plot (solid squares in the main figure). We see that, similar to our results for the diffusion constants, also this transport quantity shows at low temperatures an Arrhenius behavior which crosses over to a weaker temperature dependence with increasing temperature. In the temperature regime in which the Arrhenius law is observed the data are described very well by an Arrhenius law. If we fit the six lowest temperatures with such a law, we find an activation energy of 5.19 eV, which is in very good agreement with the experimental value of 5.33 eV.[35] By using such an Arrhenius law to extrapolate our data to lower temperatures we see that for temperatures around 2800 K such an extrapolation underestimates the viscosity of real silica, as measured by Urbain *et al.*[35] (open circles), by about a factor of 10. Thus we find that the BKS model underestimates the viscosity of real silica but that the error lies in the prefactor and not in the activation energy. (We also mention that there seems to be an uncertainty of the experimental value of the prefactor of about a factor of 2 [Ref. 54); thus it might be that the actual discrepancy between our simulation and reality is less than just stated.] We also mention that if the Arrhenius law found for our low-temperature data is used for estimating the temperature at which the viscosity of our system reaches the value 10^{13} P, i.e., the value of the experimental glass transition temperature, we find that this value is at 1310 K. Thus we find, in agreement with our results from the diffusion constant, that the BKS model underestimates the experimental glass transition temperature by about 10%.

Having an independent measurement of the diffusion constants and the viscosity, it is possible to check the validity of

the Stokes-Einstein relation in this system. This relation is given by

$$\frac{k_B T}{\eta D} = \lambda = \text{const}, \tag{12}$$

where the constant λ has, in the phenomenological Eyring theory, the meaning of a length of an elementary diffusion step.[55] To check whether the left hand side of Eq. (12) is indeed constant we plot its temperature dependence in the inset of Fig. 10. From this inset we see that λ depends in the whole temperature interval on T in that it changes from values around 20 Å at high temperatures to values around 5 Å at the lowest temperatures. This finding is not surprising in view of the fact that the activation energy of the viscosity (5.19 eV; see Fig. 10) is very close to the one of the diffusion constant of silicon (5.18 eV; see Fig. 8), thus showing that for silicon the product ηD_{Si} is constant, whereas in the Stokes-Einstein relation an additional factor T is present. Thus we conclude that in the temperature range considered here, the Stokes-Einstein relation is not a good way to convert viscosity data into diffusivities or vice versa.

From our data on the temperature dependence of the diffusion constants and the viscosity we have evidence that with increasing temperature the relaxation behavior of the system crosses over from one similar to an activated process to one which is, potentially, described well by the ideal version of MCT. On the other hand, the ideal version of the theory predicts a power-law divergence to infinity of D and η at T_c, which in our case is at 3330 K, while Figs. 8 and 10 show that this is not the case. Thus the need for the extended version of MCT is evident. Further support for a change of the transport mechanisms is obtained by investigating the temperature dependence of the lifetime of a bond between a silicon and an oxygen atom. From Fig. 2(b) we see that even at the highest temperature there is a well-defined minimum between the first and second neighbor peaks in the radial distribution function $g(r)$ for the Si-O correlation. Hence it is quite natural to make the definition that a silicon and an oxygen atom are bonded if their separation is less than the location of this minimum, which we located at 2.35 Å. In Fig. 11 we show $P_B(t)$, the probability that a bond which was present at time zero is still present at time t. From this figure we see that the decay time of this probability increases fast with decreasing temperature. More interesting is the observation that at low temperatures $P_B(t)$ does not decay to zero within the time span of our simulation, but that the curves end at around a value of 0.2. In Fig. 7 we have shown that our simulations have been long enough to allow to observe the diffusive regime in the mean-squared displacement, and in Refs. 26 and 47 we show that also the structural correlation functions, such as the intermediate scattering functions $F_s(q,t)$ and $F(q,t)$ at the FSDP,[51] decay to zero within the time span of our simulation. Hence we conclude that in order to become diffusive or for the decay of the mentioned structural correlation functions, it is not necessary that all of the bonds between silicon and oxygen break.[56]

From the figure one also sees that the shape of the curves does not seem to depend on temperature. This can be checked by plotting $P_B(t)$ versus t/τ_B, where the ''lifetime'' $\tau_B(T)$ is defined by requiring that $P_B(\tau_B) = e^{-1}$. In the inset of Fig. 11 we show this type of plot and we see that the curves for the different temperatures fall indeed very well on top of each other. At short and intermediate times the master curve is approximated well by a Kohlrausch-Williams-Watts (KWW) curve, $\exp[-(t/\tau_B)^{\beta}]$, with $\beta = 0.90$ (dashed line) decay at short times and a power-law decay at long times.

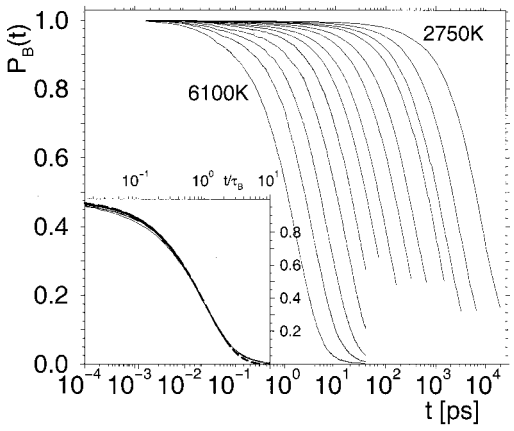

FIG. 11. Time dependence of P_B, the probability that a bond between a silicon and an oxygen atom which exists at time zero is also present at time t, for all temperatures investigated (main figure). Inset: the same data vs the rescaled time t/τ_B, where $\tau_B(T)$ is the decay time of P_B. The dashed line is a fit with a KWW law with $\beta = 0.90$.

In order to find out how the breaking of the bonds is related to the diffusion process we plot in Fig. 12 the product of the lifetime τ_B and the diffusion constants versus the inverse temperature. From this figure we recognize that the product $\tau_B D_O$ is essentially independent of temperature, demonstrating that the breaking of the bond is indeed related to the elementary diffusion step of the oxygen atoms. For the silicon atoms the situation is more complicated in that the product $\tau_B D_{\mathrm{Si}}$ is constant at high temperatures but then starts to decrease at low temperatures. Thus we have evidence that at high temperatures the diffusion mechanism for the silicon atoms is very similar to the one of the oxygen atoms and is likely governed by the collective motion described by MCT. When the system enters the Arrhenius regime the situation changes in that now the silicon atoms see a quite different

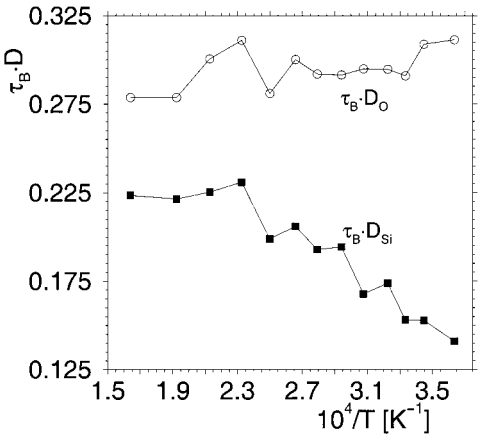

FIG. 12. Temperature dependence of the products of the diffusion constants with the decay time of P_B.

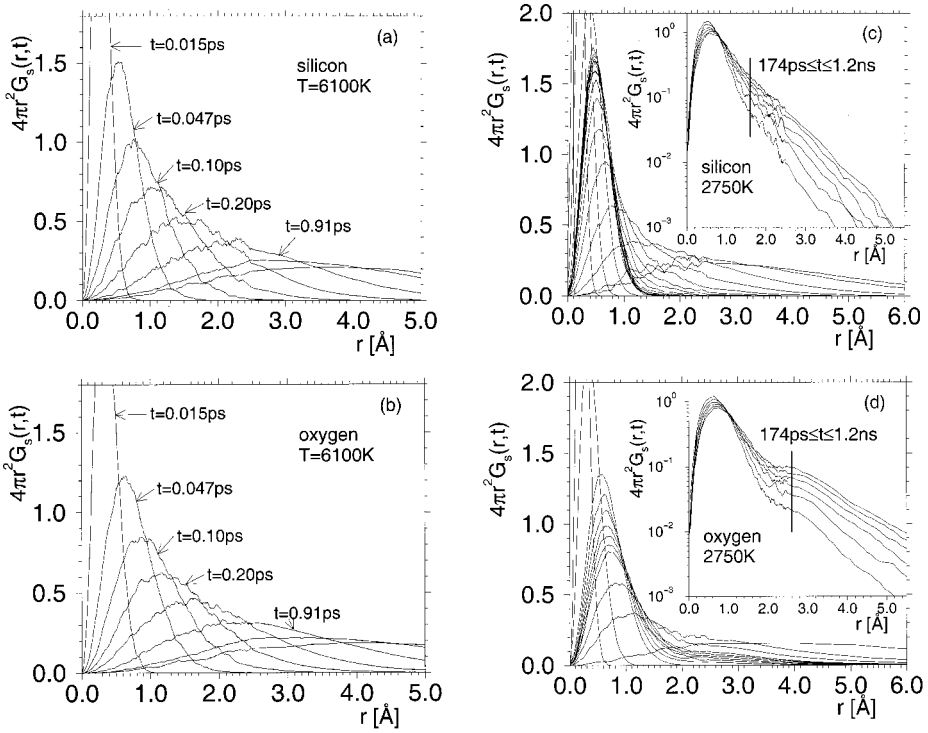

FIG. 13. Space and time dependence of the self-part of the van Hove correlation function. (a) Silicon at 6100 K, (b) oxygen at 6100 K, and (c) silicon at 2750 K. The vertical line in the inset corresponds to 1.6 Å, the length of a Si-O bond. (d) Oxygen at 2750 K. The vertical line at 2.6 Å in the inset corresponds to the nearest neighbor O-O distance. In panels (a) and (b) the times increases by about a factor of 2 from one curve to the other. In panels (c) and (d) the times are 0.015 ps, 0.033 ps, 0.38 ps, 174 ps, 362 ps, 590 ps, 817 ps, 1.04 ns, 1.2 ns, 4.5 ns, and 15.4 ns.

local (mean) potential than the oxygen atoms (since the former sit in deeper minima) and thus their diffusion motion is not directly related to the breaking of the bond with one of its neighbors.

A more detailed picture of the change of the transport mechanism can be obtained by investigating the self part of the van Hove correlation function $G_s(r,t)$[51] which is defined by

$$G_s^\alpha(r,t)=\frac{1}{N_\alpha}\sum_{i=1}^{N_\alpha}\langle\delta(r-|\mathbf{r}_i(t)-\mathbf{r}_i(0)|)\rangle,\quad \alpha\in\{\mathrm{Si,O}\}. \tag{13}$$

Thus $4\pi r^2 G_s^\alpha(r,t)$ is the probability to find a particle at time t a distance r away from the place it was at $t=0$. In Fig. 13 we show this probability for different times for $T=6100$ K and $T=2750$ K. From the figures at the higher temperature we see that the space and time dependence of $4\pi r^2 G_s^\alpha$ is very regular in that with increasing time the location of the peak moves continuously to larger distances. At this temperature no significant qualitative difference between the curves for the silicon and oxygen atoms is observed, thus showing that the transport mechanism of the two types of particles is very similar.

At low temperatures the situation is quite different. After the ballistic motion of the ions, during which the r and t dependence of G_s^α is qualitatively similar to the one at high temperatures, the distribution function shows a peak whose location depends only weakly on time. Such a behavior is well known from studies of the dynamics of supercooled liquids and is a manifestation of the cage effect discussed above.[17,19] With increasing time the height of this peak decreases and to the left of the peak a long tail is observed in the case of silicon and a small peak in the case of oxygen (around 2.6 Å). This peak can be seen better in a linear-logarithmic representation of the curves, which is shown in the insets of the figures. In their simulation of a soft-sphere system Roux *et al.*[17] related the existence of such a peak to the presence of hopping processes and thus we have direct evidence that such processes exist in the present system as well. Also included in the figure for the oxygen is the location of the first peak in the radial distribution function of the O-O correlation at 2.6 Å (vertical line), and we see that this location coincides with the location of the secondary peak in $4\pi r^2 G_s^{\mathrm{O}}(r,t)$. (We also mention that most of the oxygen atoms jumping are defects in that they are only onefold or threefold coordinated.[30])

For silicon the situation is different in that no secondary peak is visible at any time. However, a careful inspection of the curves reveals that at around 1.6 Å, marked in the inset by a vertical line, a change in the slope of the curves can be noticed. This distance corresponds to the Si-O bond in one tetrahedron. From Fig. 3(a) we see that there are still quite a few fivefold, coordinated silicon atoms in the melt and we have found that at low temperatures the transport of the particles often involves such fivefold-coordinated silicon atoms.[30] Thus a typical bond-breaking process involves a onefold-coordinated oxygen atom attaching itself to a fourfold-coordinated silicon atom, thus moving the latter by a distance of the order of half the Si-O bond length. Shortly after this, the now fivefold-coordinated silicon atom breaks the bond with one of its five nearest neighbors, thus creating

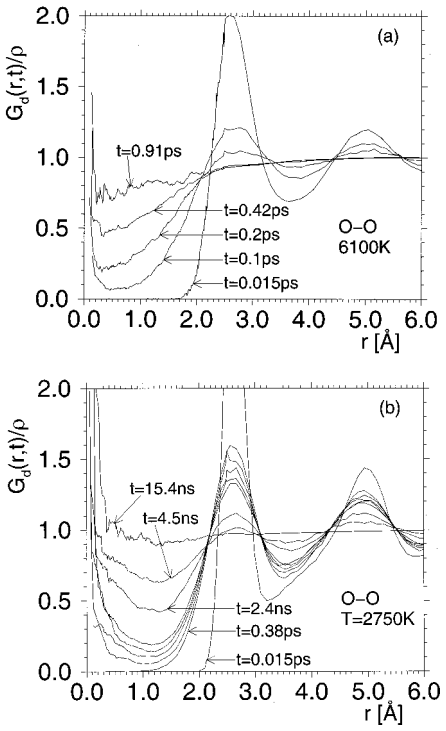

FIG. 14. Space and time dependence of the distinct part of the van Hove correlation function for the O-O pair. (a) $T=6100$ K, (b) $T=2750$ K. In panel (b) the curves that are not labeled correspond to times 174 ps, 362 ps, 590 ps, and 1.2 ns.

a new onefold-coordinated oxygen atom, and moves again on the order of half a bond length. Thus in this whole process the silicon atom has moved on the order of the length of a Si-O bond and hence $4\pi r^2 G_s^{\mathrm{Si}}(r,t)$ shows at this distance the mentioned feature.

Finally we mention that we have also investigated the space and time dependence of the distinct part of the van Hove correlation function $G_d(r,t)$ (Refs. 19 and 51) and found that this dependence is compatible with our discussion of the self-part $G_s^{\alpha}(r,t)$. This is demonstrated in Fig. 14 where we show $G_d(r,t)$ for the O-O pair at 6100 K and 2750 K. From Fig. 14(a) we see that, even at $T=6100$ K, $G_d(r,t)$ shows at intermediate times a small peak at the origin, $r=0$, thus showing that the correlation hole that is observed at time zero is filled up not only by a continuous influx from other oxygen atoms but to some extent also by particles which hop directly into the position of the oxygen atom which was there at time zero. This type of dynamics is not observed in simple liquids at high temperatures[16–18] and is thus probably attributable to the fact that silica forms a well-defined network even at high temperatures, thus making the correlation hole relatively stable and hence permitting a new oxygen atom to jump into it. We emphasize, however, that at these high temperatures this jump mechanism is not the dominant transport mechanism, since the self-part of the van Hove function does not show a secondary peak [see Fig. 13(b)].

In Fig. 14(b) we see that at low temperatures the peak at the origin is very pronounced at intermediate times and is even observable at $t=15.4$ ns, i.e., at times at which the particles show a diffusive behavior [see Fig. 7(b)]. This shows that even on these very long time scales the local structure of the network still has some resemblance to the one at time zero and that the motion of the atoms is indeed given by the hopping of the atoms in this structure.

IV. SUMMARY AND CONCLUSIONS

In this paper we have discussed the results of a large scale molecular dynamics computer simulation of a silica melt. The potential used is the one proposed by van Beest *et al.*[22] which has been found in previous simulations[23] to be quite reliable with respect to reproducing structural properties of amorphous silica at temperatures below the glass transition temperature. In the present work we focus on the structural and dynamical quantities in the *equilibrium* melt. Apart from thermodynamic quantities like the pressure and the compressibility, we have determined the partial structure factors. From these functions we conclude that the melt is substantially ordered even at temperatures as high as 6100 K and shows intermediate range order (first sharp diffraction peak) already at around 4000 K. Evidence that this high degree of local ordering is not just an artifact of our model is given first by the fact that at these temperatures the viscosity of real silica is surprisingly high,[35] thus showing that the motion of the atoms is strongly hindered because of the cage effect, and second by our finding that, if we cool the system to a temperature at which the structure can be measured, we find that the structure predicted by the simulation agrees very well with the experimental neutron scattering function $S_n(q)$, thus showing that the structure of the model is very realistic.

From the mean-squared displacement of the particles we calculate the diffusion constants D and find that at low temperatures they show an Arrhenius dependence with activation energies which agree very well with the ones found in experiments. If this temperature dependence is extrapolated to values of D which correspond to the diffusion constants of real silica around the *experimental* glass transition temperature T_g, we find that these values of D are at temperatures which agree with T_g to within 10%. A similar result is obtained from the viscosity data. Thus we conclude that the model used is very reliable to predict the relaxation behavior of real silica and is even able to predict the real glass transition temperature with surprising accuracy.

For temperatures higher than 3200 K we find significant deviations from the Arrhenius dependence of D. In that temperature range the diffusion constants are fitted much better by a power law $D\propto(T-T_c)^{\gamma}$, a temperature dependence which is often found in simple liquids and which has been proposed by mode-coupling theory. The critical temperature T_c is 3330 K, in excellent agreement with extrapolations by Hess *et al.* of experimental data.[44] A similar conclusion can be drawn from the temperature dependence of the viscosity. Thus we find that the relaxation dynamics of this system shows a crossover from a dynamics at high temperatures which can be described by the ideal version of MCT to an activated dynamics at low temperatures. The existence of this crossover can also be seen in the temperature dependence of the product of the diffusion constants and the lifetime of a Si-O bond. This product is constant in the high-temperature regime for silicon and oxygen, whereas it shows a significant (Arrhenius) temperature dependence for silicon at low temperatures, hence giving evidence for a change of

the diffusion mechanism with decreasing temperature.

As has been shown elsewhere,[57] even the activated dynamics at low temperatures can be understood to a good part within the framework of MCT, since predictions of the theory like the factorization property or the existence of the von Schweidler law[3] seem to hold very well. Thus we come to the conclusion that one of the main differences between strong and fragile glass formers is that in the former the so-called hopping processes, which invalidate some of the predictions of the *ideal* version of MCT, are, *at* T_c, very pronounced in strong glass formers. Due to the strong presence of these hopping processes, important predictions of the ideal MCT, like the presence of a power-law dependence of the transport coefficients, are valid only in a very restricted temperature range. Therefore it is important that in the analysis of the relaxation dynamics of strong glass formers those predictions of MCT are checked which are not affected by the presence of such hopping processes, if one wants to make a real test whether or not MCT is able to describe the relaxation dynamics of such a system.

ACKNOWLEDGMENTS

We thank K. Binder for many stimulating discussions on this work, J.-L. Barrat for pointing out Refs. 52 and 53 to us, and J. Baschnagel for useful discussions. This work was supported by BMBF Project No. 03 N 8008 C and by SFB 262/D1 of the Deutsche Forschungsgemeinschaft. We also thank the HLRZ Jülich for a generous grant of computer time on the T3E.

[1] See, e.g., the review article by H. Sillescu, J. Non-Cryst. Solids **243**, 81 (1999).

[2] J.-P. Bouchaud, L. F. Cugliandolo, J. Kurchan, and M. Mézard, Physica A **226**, 243 (1996); in *Spin Glasses and Random Fields*, edited by A. P. Young (World Scientific, Singapore, 1998), p. 161.

[3] W. Götze, in *Liquids, Freezing and the Glass Transition*, Proceedings of the Les Houches Summer School of Theoretical Physics, Session LI, 1989, edited by J.-P. Hansen, D. Levesque, and J. Zinn-Justin (North-Holland, Amsterdam, 1991), p. 287; W. Götze and L. Sjögren, Rep. Prog. Phys. **55**, 241 (1992); W. Kob, in *Experimental and Theoretical Approaches to Supercooled Liquids: Advances and Novel Applications*, edited by J. Fourkas, D. Kivelson, U. Mohanty, and K. Nelson (ACS Books, Washington, D.C., 1997), p. 28; W. Götze, J. Phys.: Condens. Matter **11**, A1 (1999).

[4] W. van Megen and P. N. Pusey, Phys. Rev. A **43**, 5429 (1991); E. Bartsch, M. Antonietti, W. Schupp, and H. Sillescu, J. Chem. Phys. **97**, 3950 (1992); W. van Megen and S. M. Underwood, Phys. Rev. E **49**, 4206 (1994).

[5] W. Petry, E. Bartsch, F. Fujara, M. Kiebel, H. Sillescu, and B. Farago, Z. Phys. B **83**, 175 (1991); M. Kiebel, E. Bartsch, O. Debus, F. Fujara, W. Petry, and H. Sillescu, Phys. Rev. B **45**, 10 301 (1992); A. Tölle, H. Schober, J. Wuttke, and F. Fujara, Phys. Rev. E **56**, 809 (1997); H. Z. Cummins, G. Li, W. Du, Y. H. Hwang, and G. Q. Shen, Prog. Theor. Phys. Suppl. **126**, 21 (1997); A. Tölle, J. Wuttke, H. Schober, O. G. Randl, and F. Fujara, Eur. Phys. J. B **5**, 231 (1998).

[6] J. Wuttke, J. Hernandez, G. Li, G. Coddens, H. Z. Cummins, F. Fujara, W. Petry, and H. Sillescu, Phys. Rev. Lett. **72**, 3052 (1994); J. Wuttke, W. Petry, G. Coddens, and F. Fujara, Phys. Rev. E **52**, 4026 (1995).

[7] C. A. Angell, in *Relaxation in Complex Systems*, edited by K. L. Ngai and G. B. Wright (U.S. Department of Commerce, Springfield, MA, 1985).

[8] D. Sidebottom, R. Bergman, L. Börjesson, and L. M. Torell, Phys. Rev. Lett. **71**, 2260 (1993).

[9] A. Wischnewski, U. Buchenau, A. J. Dianoux, W. A. Kamitakahara, and J. L. Zarestky, Phys. Rev. B **57**, 2663 (1998).

[10] See, e.g., references in C. A. Angell, J. H. R. Clarke, and L. V. Woodcock, Adv. Chem. Phys. **48**, 397 (1981); W. Kob, in *Annual Reviews of Computational Physics*, edited by D. Stauffer (World Scientific, Singapore, 1995), Vol. III, p. 1; W. Kob, J. Phys.: Condens. Matter **11**, R85 (1999).

[11] J. Habasaki, I. Okada, and Y. Hiwatari, Phys. Rev. E **52**, 2681 (1995); R. Dell'Anna, G. Ruocco, M. Sampoli, and G. Viliani, Phys. Rev. Lett. **80**, 1236 (1998).

[12] S. N. Taraskin and S. R. Elliott, Europhys. Lett. **39**, 37 (1997); Phys. Rev. B **56**, 8605 (1997).

[13] J. Horbach, W. Kob, and K. Binder, J. Non-Cryst. Solids **235-238**, 320 (1998).

[14] U. Buchenau, M. Prager, N. Nücker, A. J. Dianoux, N. Ahmed, and W. A. Phillips, Phys. Rev. B **34**, 5665 (1986); P. Benassi, M. Krisch, C. Masciovecchio, V. Mazzacurati, G. Monaco, G. Ruocco, F. Sette, and R. Verbeni, Phys. Rev. Lett. **77**, 3835 (1996); M. Foret, E. Courtens, R. Vacher, and J.-B. Suck, *ibid.* **77**, 3831 (1996); W. Schirmacher, G. Diezemann, and C. Ganter, *ibid.* **81**, 136 (1998).

[15] J. R. Rustad, D. A. Yuen, and F. J. Spera, Phys. Rev. B **44**, 2108 (1991); W. Jin, R. K. Kalia, P. Vashishta, and J. P. Rino, Phys. Rev. Lett. **71**, 3146 (1993); J. P. Rino, I. Ebbsjö, R. K. Kalia, A. Nakano, and P. Vashishta, Phys. Rev. B **47**, 3053 (1993); Y. Guissani and B. Builolot, J. Chem. Phys. **104**, 7633 (1996); P. H. Poole, M. Hemmati, and C. A. Angell, Phys. Rev. Lett. **79**, 2281 (1997); J. Badro, P. Gillet, and J.-L. Barrat, Europhys. Lett. **42**, 643 (1998); M. Wilson and P. A. Madden, Phys. Rev. Lett. **80**, 532 (1998).

[16] B. Bernu, J.-P. Hansen, Y. Hiwatari, and G. Pastore, Phys. Rev. A **36**, 4891 (1987); H. Miyagawa, Y. Hiwatari, B. Bernu, and J.-P. Hansen, J. Chem. Phys. **88**, 3879 (1988); J.-L. Barrat, J.-N. Roux, and J.-P. Hansen, Chem. Phys. **149**, 197 (1990); H. Miyagawa and Y. Hiwatari, Phys. Rev. A **44**, 8278 (1991).

[17] J. N. Roux, J.-L. Barrat, and J.-P. Hansen, J. Phys.: Condens. Matter **1**, 7171 (1989).

[18] W. Kob and H. C. Andersen, Phys. Rev. Lett. **73**, 1376 (1994); Phys. Rev. E **52**, 4134 (1995).

[19] W. Kob and H. C. Andersen, Phys. Rev. E **51**, 4626 (1995).

[20] P. Gallo, F. Sciortino, P. Tartaglia, and S.-H. Chen, Phys. Rev. Lett. **76**, 2730 (1996); S.-H. Chen, P. Gallo, F. Sciortino, and P. Tartaglia, Phys. Rev. E **56**, 4231 (1997); F. Sciortino, L. Fabbian, S.-H. Chen, and P. Tartaglia, *ibid.* **56**, 5397 (1997).

[21] M. Hemmati and C. A. Angell, in *Physics Meets Geology*, edited by H. Aoki and R. Hemley (Cambridge University Press, Cambridge, England, 1998).

[22] B. W. H. van Beest, G. J. Kramer, and R. A. van Santen, Phys. Rev. Lett. **64**, 1955 (1990).
[23] K. Vollmayr, W. Kob, and K. Binder, Phys. Rev. B **54**, 15 808 (1996).
[24] K. Vollmayr and W. Kob, Ber. Bunsenges. Phys. Chem. **100**, 1399 (1996).
[25] J. Horbach, W. Kob, K. Binder, and C. A. Angell, Phys. Rev. E **54**, R5897 (1996).
[26] J. Horbach, W. Kob, and K. Binder, Philos. Mag. B **77**, 297 (1998).
[27] J. Horbach, W. Kob, and K. Binder, J. Phys. Chem. B **103**, 4104 (1999).
[28] R. Brückner, J. Non-Cryst. Solids **5**, 123 (1970).
[29] M. P. Allen and D. J. Tildesley, *Computer Simulation of Liquids* (Oxford University Press, New York, 1990).
[30] J. Horbach, Ph.D. thesis, University of Mainz, 1998.
[31] Probably this drift originates in the discontinuity of the potential at 5.5 Å.
[32] J.-P. Hansen and I. R. McDonald, *Theory of Simple Liquids* (Academic, London, 1986).
[33] A. Roder, W. Kob, and K. Binder (unpublished).
[34] K. Vollmayr, Ph.D. thesis, University of Mainz, 1995.
[35] G. Urbain, Y. Bottinga, and P. Richet, Geochim. Cosmochim. Acta **46**, 1061 (1982).
[36] S. Susman, K. J. Volin, D. G. Montague, and D. L. Price, Phys. Rev. B **43**, 11 076 (1991).
[37] D. L. Price and J. M. Carpenter, J. Non-Cryst. Solids **92**, 153 (1987).
[38] We remind the reader that the glass at 300 K was produced by cooling the system from 2900 K.
[39] D. B. Fraser, J. Appl. Phys. **39**, 5868 (1968).
[40] C. A. Angell, P. H. Poole, and J. Shao, Nuovo Cimento D **16**, 993 (1994).
[41] E. Rössler, A. P. Sokolov, A. Kisliuk, and D. Quitmann, Phys. Rev. B **49**, 14 967 (1994).
[42] J. C. Mikkelsen, Appl. Phys. Lett. **45**, 1187 (1984).
[43] G. Brébec, R. Seguin, C. Sella, J. Bevenot, and J. C. Martin, Acta Metall. **28**, 327 (1980).
[44] K.-U. Hess, D. B. Dingwell, and E. Rössler, Chem. Geol. **128**, 155 (1996); E. Rössler, K.-U. Hess, and V. N. Novikov, J. Non-Cryst. Solids **223**, 207 (1998).
[45] M. Nauroth and W. Kob, Phys. Rev. E **55**, 657 (1997).
[46] S. Kämmerer, W. Kob, and R. Schilling, Phys. Rev. E **56**, 5450 (1997); **58**, 2131 (1998); **58**, 2141 (1998).
[47] J. Horbach and W. Kob (unpublished).
[48] S. P. Das and G. F. Mazenko, Phys. Rev. A **34**, 2265 (1986); W. Götze and L. Sjögren, Z. Phys. B **65**, 415 (1987); M. Fuchs, W. Götze, S. Hildebrand, and A. Latz, J. Phys.: Condens. Matter **4**, 7709 (1992).
[49] T. Gleim, W. Kob, and K. Binder (unpublished).
[50] J.-L. Barrat, J. Badro, and P. Gillet, Mol. Simul. **20**, 17 (1997).
[51] J. P. Boon and S. Yip, *Molecular Hydrodynamics* (Dover, New York, 1980).
[52] M. P. Allen, D. Brown, and A. J. Masters, Phys. Rev. E **49**, 2488 (1994); M. P. Allen, *ibid.* **50**, 3277 (1994).
[53] J. Alejandre, D. J. Tildesley, and G. A. Chapela, J. Chem. Phys. **102**, 4574 (1995); D. M. Heyes, Phys. Rev. B **49**, 755 (1994).
[54] O. V. Mazurin, M. V. Streltsina, and T. P. Shvailko-Shvailkovskaya, *Handbook of Glass Data, Part A: Silica Glass and Binary Silicate Glasses* (Elsevier, Amsterdam, 1983).
[55] S. Glasstone, K. J. Laidler, and H. Eyring, *The Theory of Rate Processes* (McGraw-Hill, New York, 1941).
[56] We mention that this is the case at high temperatures also. However, since at these temperatures the relaxation times τ are short, our runs were so long, compared to τ, that in the time span of the simulation even $P_B(t)$ decays to zero.
[57] W. Kob, J. Horbach, and K. Binder, *Slow Dynamics in Complex Systems*, edited by M. Tokoyama and I. Oppenheim (AIP, Woodbury, NY, 1999).